Polyvinyl Alcohol-Cellulose Nanocrystal Hydrogel Containing Anti-inflammatory Agent

Lia Amelia Tresna Wulan Asri[1*], Athiya Anindya[1], Yuni Eva Kartika[1], Dita Puspitasari[1], Untung Triadhi[2], and Husaini Ardy[1]

[1]*Materials Science and Engineering Research Group, Faculty of Mechanical and Aerospace Engineering, Institut Teknologi Bandung, Jl. Ganesha No. 10, Bandung 40132, Indonesia*

[2]*Analytical Chemistry Division, Department of Chemistry, Faculty of Mathematics and Natural Sciences, Institut Teknologi Bandung, Jl. Ganesha No. 10, Bandung 40132, Indonesia*

* ***Corresponding author:***

email: lia.asri@material.itb.ac.id

Received: March 2, 2022
Accepted: July 4, 2022

DOI: 10.22146/ijc.73357

Abstract: *Hydrogel wound dressings were developed through cross-linking reactions of polyvinyl alcohol (PVA) with glutaraldehyde and by the addition of diclofenac sodium and rutin as anti-inflammatory agents. Cellulose nanocrystals (CNC) were added to improve mechanically and release properties. CNC was isolated from pineapple leaf fibers through the ammonium persulfate method resulting in a mixture of rod-like whisker and spherical morphology. The mechanical properties of hydrogels are increasing with the addition of CNC. Hydrogels containing 8% CNC exhibited 7.266 N/mm^2 tensile strength, 156.3% maximum strain, and 700.3 N/mm^2 elastic modulus. Drug release tests containing sodium diclofenac were done by taking incubated phosphate buffer saline samples in a pH 7.4 environment and showed that all CNC variations tested are controllable for the first 30 min compared to the sample without CNC. Sodium diclofenac is easily eluted from hydrogel due to its polar properties, and all samples almost demonstrated the same release profile. PVA hydrogels showed fluctuating concentrations of diclofenac compared to others. While hydrogels containing rutin showed a controlled release mode, the addition of CNC in PVA resulted in a slower release of rutin, possibly due to the better binding between CNC and rutin. To conclude, CNC has successfully improved the performance of PVA hydrogels, including the drug release properties.*

Keywords: *hydrogel; wound dressing; polyvinyl alcohol; cellulose nanocrystals; anti-inflammatory agents*

■ INTRODUCTION

A wound is a disorder that occurs in the integrity of the skin, mucous membranes, or skin tissue that can cause physical or thermal damage [1]. The wound healing process is a biological process that occurs in the human body, which includes four stages, namely hemostasis, inflammation, proliferation, and remodeling, that must be done sequentially and in the correct period [2]. When a skin injury occurs, microorganisms around the surrounding tissue would invade the wound and initiate an infection [3]. The presence of pathogens interferes with the inflammation stage and, as a result, delays the proliferation and remodeling stage which leads to tissue damage [4-5]. An infected wound takes longer to heal than the normal healing process [6]. External origin wounds such as those caused by falls or surgical procedures are caused by external force or trauma, resulting in a longer healing time and a higher cost of care. Therefore, the infection must be avoided to ensure a successful and accelerated healing process.

Various treatments and materials are available to treat acute and chronic wounds. Conventional wound care involves drying the area of injury with gauze and tulle by absorbing moisture. This type of dressing provided some protection from the external environment. On the other hand, advanced wound dressing promoted active healing by providing moisture and allowing therapeutic agents to be released in a

controlled manner [7-8]. Therefore, appropriate wound dressing material is necessary to ensure moisture, drug entrapment, and its release [9-10].

Hydrogels, for example, are one type of commercial wound dressing that promotes a moist environment. Hydrogels are hydrophilic polymers that help wounds stay moist while absorbing exudate and can be blended with active compounds such as antibacterial agents due to their versatility [10-13]. They also have a porous structure that holds high water content [14]. The development of hydrogels has been studied extensively, and their commercial use for biomedical applications is developing [15].

Some widely used polymers, including polyvinyl alcohol (PVA) [12,14], polyvinylpyrrolidone (PVP) [16-17], and polyethylene glycol (PEG) [18-19], have low mechanical, thermal, and barrier properties [10]. As a result, nanoparticles are frequently used to improve their properties. Nanocellulose is favored as hydrogel reinforcement because of its functional drug release capabilities, high air-holding capacity, high crystallinity, and biocompatibility [20-22]. Cellulose comprises β-1,4-linked glucopyranose monomers joined by glycosidic bonds [23]. The presence of three hydroxyl groups in each monomer contributes to forming strong hydrogen bonds.

Cellulose nanocrystals (CNCs) consist of highly crystalline regions (54–88% crystallinity) and have a rod-like shape or whisker with 2–20 nm in diameter and 100–500 nm in length [24]. Several methods are available to extract the crystalline regions of cellulose to create CNCs, including acid hydrolysis [25], an ultrasonic technique [26], and enzymatic hydrolysis [27]. Acid hydrolysis by sulfuric acid introduces sulfate groups to the surface of CNCs due to the esterification of hydroxyl groups [25]. The high density of hydroxyl groups in cellulose increases the surface modification options of CNCs. Isogai et al. [28] have demonstrated that carboxyl groups (carboxylated CNCs) can be created by the TEMPO-mediated oxidation method. The addition of carboxyl groups weakens hydrogen bonding and increases adsorption capability, allowing carboxylated CNCs to be used as drug-carrying hydrogels.

On the other hand, TEMPO-mediated oxidation requires many steps and a long oxidation time, while periodate-chlorite oxidation to make carboxylated CNCs involves a two-step procedure that needs expensive periodate. Recently, ammonium persulfate (APS) has successfully extracted CNCs with higher carboxyl content and more homogenous rod-like particles [21]. Although it is time-consuming, this method is a one-step procedure. Thus, APS hydrolysis was used to make carboxylated CNCs in this study.

Permeability to oxygen and rapid dehydration remain the main issues of hydrogel wound dressings [29]. Therefore, determining the water content is critical, and in the current research, hydrogels with various CNC concentrations and anti-inflammatory agents rutin and diclofenac sodium will be used. The modified hydrogels' functional groups, tensile properties, water content, and drug release profiles were assessed.

■ EXPERIMENTAL SECTION

Materials

PVA, diclofenac sodium, glutaraldehyde, and rutin hydrate were purchased from Sigma-Aldrich. APS 98% and sodium hydroxide (NaOH) from Merck were used. Phosphate buffer saline (PBS) pH 7.4 and sodium hypochlorite (NaOCl, technical grade 12%) were supplied by Biogear and Brataco, respectively. Pineapple leaf fiber was purchased from Inatex. All chemicals were used without further purification.

Instrumentation

Fourier-transform infrared spectroscopy (FTIR) was used to determine the functional groups of CNC and hydrogels. FTIR spectra were recorded on an FTIR spectrometer (Prestige 21, Shimadzu) using the KBr pressed-pellet method. The spectra were measured at a resolution of 4 cm^{-1} with the number of scans of 40, at wavenumber 4500 to 400 cm^{-1}.

Transmission Electron Microscopy (TEM) was used to study CNC morphology. The specimen was prepared by dispersing a small amount of CNC in ethanol on a carbon-coated Cu-grid substrate and leaving

it at room temperature for approximately 15 min. TEM images were taken using HITACHI HT7700 with an 80–100 kV acceleration voltage.

The crystal structure of the CNC was studied using X-ray Diffraction (XRD) on an X-ray diffractometer (D8 ADVANCE, Bruker) using Cu Ka X-rays (λ = 0.154060 nm) with a voltage of 40 kV and a current of 40 mA. The data were collected over the 2θ range of 10–60°. The crystallinity index (CI) was calculated using the following equation:

$$Cl(\%) = \frac{I_{002} - I_{am}}{I_{002}} \times 100\% \quad (1)$$

where I_{002} is the intensity for the crystalline cellulose (2θ = 22.5°) and I_{am} is the intensity for the amorphous cellulose (2θ = 18°).

A tensile test was performed on a hydrogel sample shaped into dog bone. The test was conducted using Shimadzu with a maximum load of 1 kN and 10 mm/min velocity. Values of elastic modulus, maximum strain, and ultimate tensile strength were recorded.

Procedure

Isolation of CNC from pineapple leaf fiber

CNC was isolated from pineapple leaf fiber through a modified procedure [21,30]. Pineapple fibers were cut into small pieces. Fibers (40 g) were added into 600 mL NaOH 4 M solution and stirred at 80 °C for 4 h to remove lignin from the cellulosic fibers. The resulting suspension was washed with demineralized water several times until pH 7. The semi-dried fibers were left in the oven at 60 °C for 12 h, bleached using 1.3 L of 5% NaOCl, and heated at 80 °C for 4 h afterward. The resulting suspension was then rewashed with demineralized water until neutral pH. Next, semi-dried fibers were left at 60 °C for another 8 h in the oven. The fibers were then treated with 1.3 L APS 1 M at 80 °C for 16 h and washed with demineralized water several times until the filtrate reached pH 7.

Preparation of PVA-CNC hydrogel

Four hydrogel samples containing 0, 2, 4, and 8% CNC (Table 1) were prepared following Tanpichai et al. [22]. CNC suspension was diluted with distilled water to obtain a total of 100 mL colloidal solution with various concentrations of wt.% CNC. PVA powder (4 g) was added to the aqueous CNC suspension to make a 4 wt.% solid content solution and continuously stirred for 3 h at 90 °C. Glutaraldehyde (5 phr) was added dropwise to the suspension and stirred for 5 min. A small amount of HCl was added to adjust the pH to 1 to initiate a crosslink in the hydrogel solution. The suspension was poured into a petri dish and left for 24 h at room temperature to form hydrogel (Fig. 1(a)). The hydrogel was repeatedly rinsed with distilled water until reaching pH 5 and stored at 5 °C before use.

Table 1. Composition of hydrogel samples

Hydrogel sample	Water (mL)	PVA (g)	CNC (g)
0% CNC	60	2.4	0
2% CNC	60	2.4	2
4% CNC	60	2.4	4.08
8% CNC	60	2.4	8.53

Preparation of PVA-CNC-Rutin hydrogel

PVA-CNC hydrogel was freeze-dried overnight. The dried hydrogel (50 mg) of each CNC concentration was dispersed in a 10 mL solution of rutin (5 mg/mL) for 24 h. Hydrogels were taken out of the solution and incubated in 100 mL PBS pH 7.4, stirred at 37 °C for 2 h. The solution was measured at 271 nm on a UV-Vis spectrophotometer to determine the rutin loading content.

Preparation of PVA-CNC-Diclofenac sodium hydrogel

CNC suspensions with concentrations of 0, 2, 4, 6, and 8% were prepared by dissolving CNC in distilled water. Then, PVA powder was added to CNC suspension with a concentration of 4 wt.% (4 g in 100 mL of colloidal solution). The resulting solution was stirred for 3 h at 90 °C and let sit at room temperature for about 1 h. Diclofenac sodium (0.06 g) was then added and stirred for 30 min without being heated. The hydrogel was cross-linked by adding glutaraldehyde (GA) solution (50 wt.% in water) dropwise with a content of 5 phr, then stirred for 5 min to homogenize it. A few drops of HCl were added to adjust the pH to 1. The 60 mL hydrogel solution was poured equally into a 15 cm diameter and left at room temperature for 24 h before being stored in the refrigerator to avoid dry hydrogel-forming when left at room temperature for too long.

Swelling test

PVA-CNC hydrogel samples (50 mg) were utterly soaked in distilled water at room temperature at a predetermined time (10, 20, 30, 60, 120, 240, 360, 720, and 1440 min). Each swollen sample was taken out and weighed immediately after adsorbing excess water on its surface with filter paper. The swelling ratio was calculated as follows:

$$\text{Swelling ration} = \frac{(W_t - W_o)}{W_o} \quad (2)$$

where W_t is the weight of the swollen sample, and W_o is the initial weight. The standard deviation value was determined in triplicate.

■ RESULTS AND DISCUSSION

Isolation of CNC

The preparation scheme of CNC from pineapple leaf fibers is shown in Fig. 1(a). Pineapple leaf fibers were treated with NaOH and NaOCl to completely remove hemicellulose and lignin. The white color of the resulting sample indicates the removal of lignin, later confirmed by FTIR analysis. Cellulose was treated with APS 1 M to result in a colloidal solution of CNC. APS at elevated temperature generates radical ions and further forms hydrogen peroxide under acid conditions. Radical ions penetrate the amorphous area of cellulose and cleave the 1,4-β bond. Radical ions and hydrogen peroxide also undergo oxidation reactions and result in COOH groups on the surface of CNC [21].

TEM images depict rod-like whisker CNC with 17–71 nm in width and 89–1436 nm in length (Fig. 2(a-c). We also observed CNC with spherical morphology with a diameter of 13–350 nm (Fig. 2(a) and 2(d)). The stability of CNC whiskers strongly depends on particle size, size polydispersity, and surface charge. Nanocellulose dimensions, sizes, and crystallinity are influenced by the acid hydrolysis conditions and cellulose source. Cheng et al. [31]. reported that the morphology of cellulose nanoparticles would shift from whisker to spherical as APS concentration increased. In our case, besides the APS concentration, the non-uniform size of pineapple leaf fiber precursor might affect

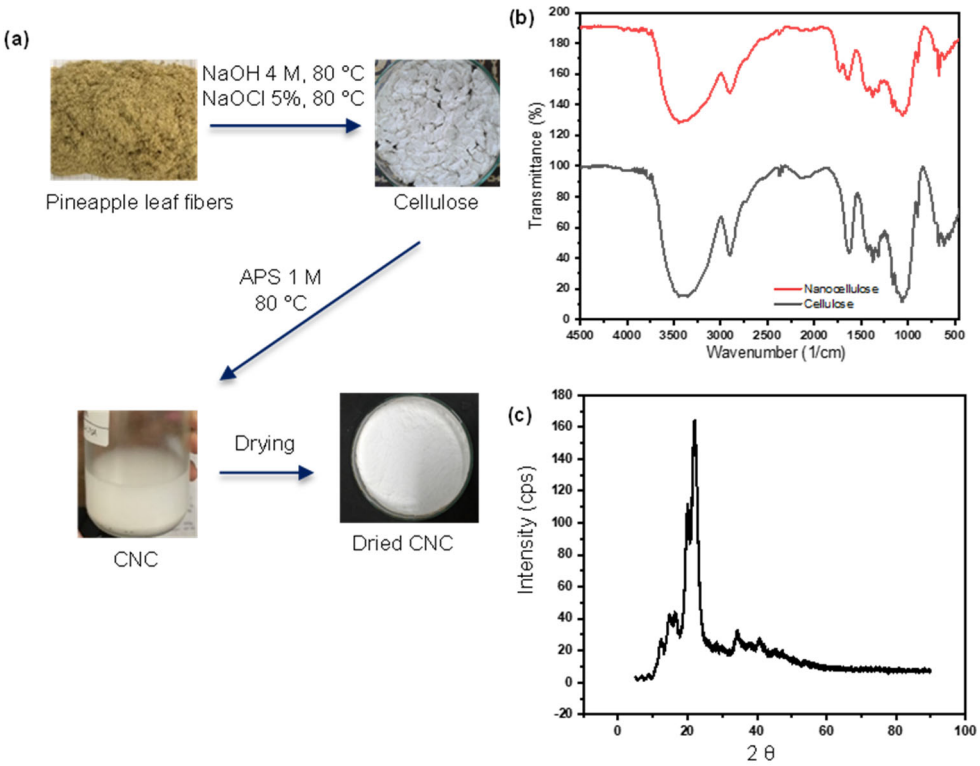

Fig 1. (a) Isolation of CNC from pineapple leaf fibers using APS method, (b) FTIR spectra and (c) XRD diffractogram of CNC

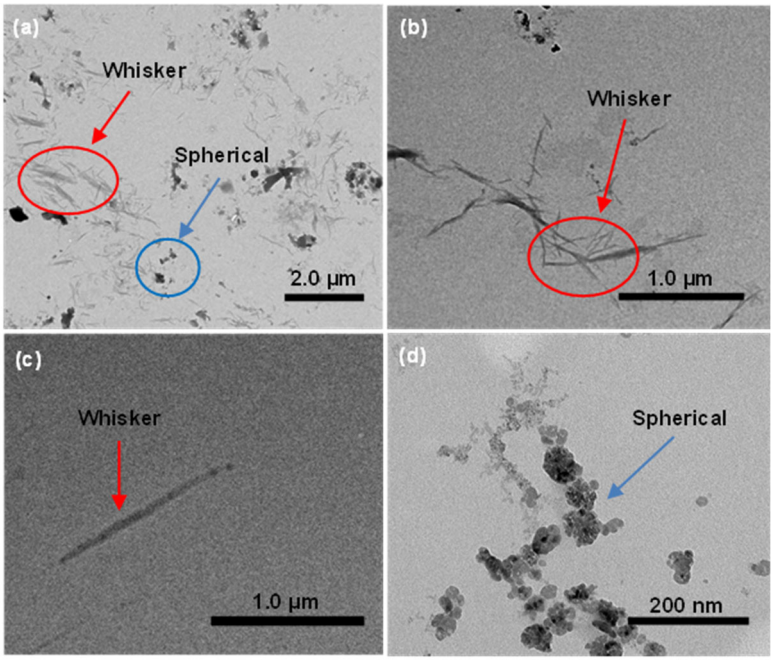

Fig 2. TEM images of CNC with (a) mixture of whisker and spherical (b, c) whisker and (d) spherical morphologies

the morphology of CNC. APS will easily react with smaller size precursors. Furthermore, the free radicals and hydrogen peroxide generated from APS not only attack the amorphous region of cellulose fibers but also hydrolyze the crystalline part. This leads to the size reduction of CNC and even morphological changes from whisker to spherical.

The FTIR spectra of CNC, as presented in Fig. 1(b), display almost similar vibrations with cellulose, as shown by vibrations at 3445 cm^{-1} (O-H hydrogen bonding), 2898 cm^{-1} (C-H asymmetric stretching), 2724 cm^{-1} (C-H symmetric stretching), 1650 cm^{-1} (O-H from adsorbed water), and 1384–1035 cm^{-1} (C-O stretching). Both cellulose and CNC show signals at 1430 cm^{-1} (CH_2 symmetric bending and OCH), 1162 cm^{-1} (C-O-C asymmetric stretching, β-glycosidic linkage), 1061 cm^{-1} (C-O/C-C stretching), and 896 cm^{-1} (asymmetric C-H out-of-plane stretching vibrations), attributed to the high content of cellulose I structure. A new band at 1726 cm^{-1} is observed in the CNC, originating from C=O stretching vibrations of carboxylic acid groups (COOH). This functional group was formed during the hydrolysis of cellulose fibers. APS was used to isolate CNC from pineapple fibers due to its rising prevalence as a strong oxidizing agent that can produce distributed rod-like whiskers without pretreatments [21,32]. The fibers were dissolved in NaOH and NaOCl solutions to remove hemicellulose and lignin before being treated with APS. The peroxide bond of APS was thermally broken when heated to 80 °C, resulting in SO_4^- free radicals and hydrogen peroxide. The radical ions penetrated the amorphous regions of cellulose and hydrolyzed the 1,4-β bond of the cellulose chain, allowing the formation of COOH groups [21].

The XRD pattern in Fig. 1(c) indicates the structure of cellulose I with main diffraction peaks at 15.1° (110), 16.4° (110), 20.9° (110), 22° (200) and 34.5° (004) [33]. The crystallinity of CNC accounted for 41.4% based on the ratio of crystalline area to the total scattered intensity and average crystallite size of 3.274 nm. Previously, we have reported CNC isolation with the APS method resulted in dominantly whisker morphology with 80% crystallinity [30]. The lack of ultrasound treatment and the inability of APS to dissolve amorphous cellulose resulted in low crystallinity. Besides, spherical CNC might contribute to lower crystallinity.

Synthesis of PVA-CNC Hydrogel

Fig. 3(a) depicts the visual of PVA-CNC with various concentrations of CNC. In general, all hydrogel

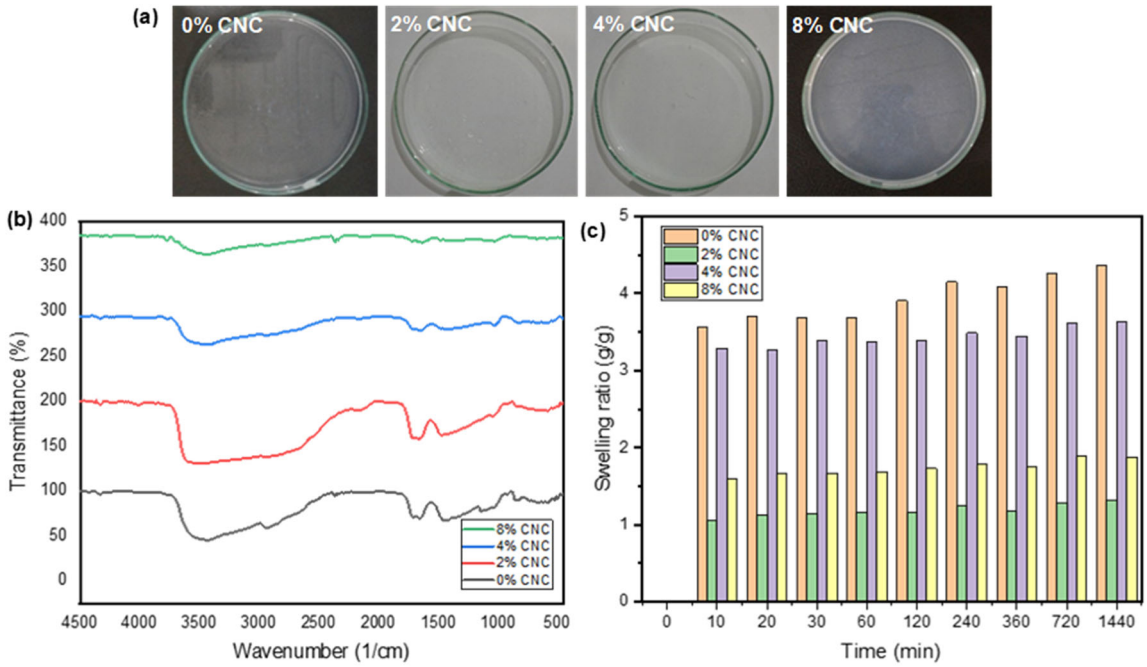

Fig 3. (a) Visual of hydrogels, (b) FTIR spectra of hydrogels and (c) Swelling ratio of PVA hydrogels with various weight concentrations of CNC

Table 2. Composition of PVA-CNC hydrogel samples loaded with diclofenac sodium

Hydrogel sample	Water (mL)	PVA (g)	CNC (g)	Diclofenac sodium (g)
Hydrogel 0% CNC	60	2.4	0	0.06
Hydrogel 2% CNC	60	2.4	2	0.06
Hydrogel 4% CNC	60	2.4	4.08	0.06
Hydrogel 8% CNC	60	2.4	8.53	0.06

variations showed no visual difference, resulting in colorless hydrogels. The FTIR spectra of various hydrogels (with and without CNCs) exhibit an almost similar profile as CNCs peaks overlap with PVA functional groups at 3430 cm^{-1} (O-H hydrogen bonding), 2935 cm^{-1} (CH_2 asymmetric stretching), 1653 cm^{-1} (C=O carbonyl stretching), 1440 cm^{-1} (C-H bending), 1031 cm^{-1} (C-O stretching) and 839 cm^{-1} (C-C stretching) as shown in Fig. 3(b). A small peak at 1139 cm^{-1} (C-O stretching) was present in PVA hydrogel, showing the characteristic of PVA.

A significant change was observed in the swelling ratio of hydrogels after immersion in water. The highest swelling ratio was found in the 0% CNC sample, while the lowest was found in the 2% CNC sample (Fig. 3(c)). In general, higher CNC content led to a lower swelling ratio. However, a notable deviation was observed in 2% CNC. The combination of PVA and CNC initiates cross-linking and hydrogen bonds formation thus reducing the number of functional groups that can bond with water molecules and decreasing the swelling ratio [22]. The observable difference in 2% CNC could be attributed to uneven CNC distribution in the hydrogel matrix and the absence of pores. FTIR test of the hydrogel sample in triplicate and pore size measurement should be carried out to determine the valid reason.

Synthesis of PVA-CNC-Diclofenac Sodium Hydrogel

PVA-CNC-diclofenac sodium hydrogels were prepared as depicted in Fig. 4. The mixture of PVA, CNC, and sodium diclofenac (Table 2) was reacted with glutaraldehyde to result in a crosslink bond between hydroxyl functional groups. The crosslink can form between PVA-PVA chains, CNC-CNC or PVA-CNC. In

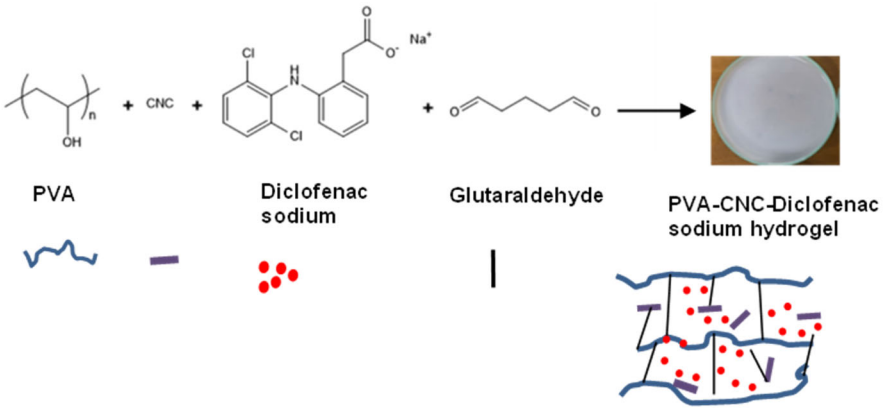

Fig 4. Synthesis of PVA-CNC-diclofenac sodium hydrogel crosslinked with glutaraldehyde

general, all hydrogel variations showed no visual difference. The white color comes from adding diclofenac sodium to the CNC solution. Due to its high water content, the hydrogel sample 0% CNC was challenging to be removed from the petri dish because the hydrogel absorbed more water during the gelling process when it was left at room temperature after mixing all materials. The hydrogel in sample 2% CNC showed a similar characteristic to the 0% CNC, which had relatively high water retention, leading it to stick to the petri dish. On the other hand, the 4, 6, and 8% CNC were more flexible and therefore, they were quickly removed from the petri dish and did not rip throughout the process.

The 8% CNC hydrogel had the highest tensile strength of 7.266 N/mm^2, while the 0% CNC hydrogel exhibited the lowest strength of 0.012 N/mm^2. Theoretically, CNC has Young's modulus value higher than microfibril cellulose (100 GPa) as CNC exhibit a higher degree of crystallinity after removal of the amorphous region [34]. CNC works as a hydrogel reinforcement, increasing the tensile strength and elastic modulus. As shown in Table 3, Young's modulus generally increased when the concentration of CNC increased. Other than that, the material and treatment of hydrogels influence the mechanical properties.

The drug release profile of 0% CNC hydrogel, as shown in Fig. 5(a), showed a significant concentration release of about 0.009 mg/mL in the first 30 min because this hydrogel did not contain CNC and CNC controls drug release. The trend continued to peak at 0.017 mg/mL in 90 min before gradually decreasing to approximately 0.0028 mg/mL concentration in 480 min. However, after 90 min, the total weight of the hydrogel (Fig. 5(b)) increased steadily, indicating that the remaining diclofenac sodium that was not cross-linked with PVA had been dissolved. The same early bursts were present in 2% CNC hydrogel, however, the release concentration in the first 5 min was 72% lower (0.0025 mg/mL) than the 0% CNC hydrogel due to CNC content in the 2% CNC hydrogel, which played a role in controlling the release of drugs from the hydrogel. In 90 min, the release peaked at 0.022 mg/mL before declining.

However, after a 5-min incubation, the release concentration on 4% CNC hydrogel was unexpectedly greater than 0 and 2% CNC hydrogels, with approximately 0 .015 mg/mL. This could be due to its

Table 3. Result of tensile test of PVA-CNC-diclofenac sodium hydrogel

Hydrogel sample	Tensile strength (MPa)	Maximum strain (%)	Young's modulus (MPa)
Hydrogel 0% CNC	0.01	76.25	191.72
Hydrogel 2% CNC	0.15	123.20	411.26
Hydrogel 4% CNC	1.53	67.48	580.03
Hydrogel 8% CNC	7.27	156.30	700.37

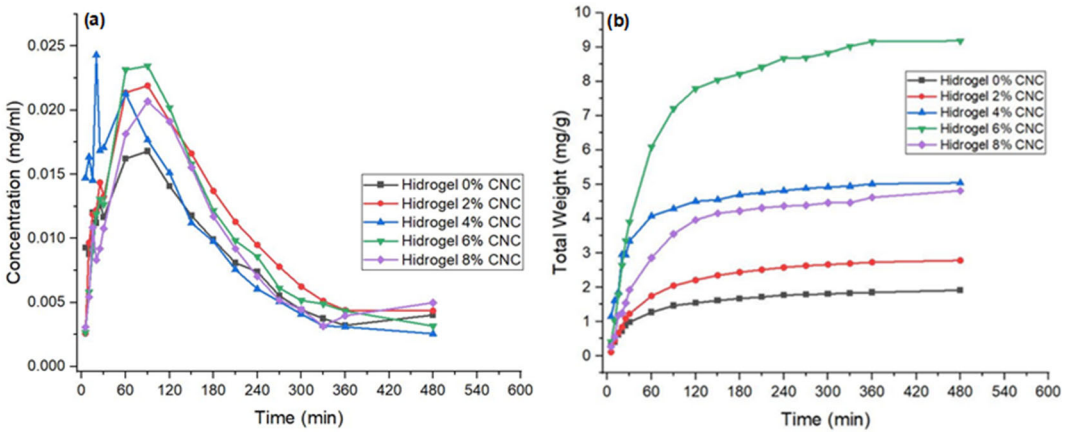

Fig 5. *In vitro* drug release of sodium diclofenac in PBS pH 7.4 (a) concentration release of rutin versus time, and (b) cumulative release ratio (mg/g) of rutin versus time

lower thickness compared to the other two hydrogels, causing more surface diclofenac sodium molecules to disperse. During the hydrogel formation process, diclofenac sodium might be trapped on the surface of the hydrogel. The concentration peaked at 0.024 mg/mL, the highest of all variants. After 60 min, the drug concentration dropped significantly, in line with the total weight profile, which remained relatively constant.

The 6% CNC hydrogel, in contrast, had a substantially lower concentration (0.002 mg/mL) than other hydrogels, indicating that CNC in the sample could effectively trap diclofenac sodium. The concentration reached a peak of 0.023 mg/mL in 90 min. As for 8% CNC hydrogel, the release concentration at the 5-min mark was slightly higher than 2% CNC hydrogel. The concentration should theoretically be lower because a higher amount of CNC should better retain drug molecules. This could be because the CNC in 8% CNC hydrogel could no longer effectively hold diclofenac sodium. Furthermore, low homogeneity of diclofenac sodium in the 8% CNC hydrogel was found.

Synthesis of PVA-CNC-Rutin Hydrogel

Hydrophobic rutin is also employed as a drug model for an anti-inflammatory agent. PVA-CNC-rutin hydrogels were prepared by crosslinking PVA and CNC with glutaraldehyde, followed by freeze-drying and drug loading in a rutin solution (Fig. 6). PVA and PVA-CNC exhibited the loading content around 4.89–4.90%.

The release profile indicates that all hydrogels performed controlled release (Fig. 7). The addition of hydrophobic rutin to 2% CNC hydrogel exhibited a significantly lower release concentration than 0% CNC hydrogel, revealing that CNC entrapment in the hydrogels affected the release of rutin. Rutin contains hydroxyl groups that can form hydrogen bonds with the hydroxyl and carboxyl groups of the hydrogel [28]. As the resulting intramolecular hydrogen bonds enhance resulting, the release concentration decrease. At the same time, the swelling ratio might also be responsible for the release behavior. A higher swelling ratio suggested that a higher rutin solution (in water) could be preserved in the hydrogel, therefore inhibiting rutin

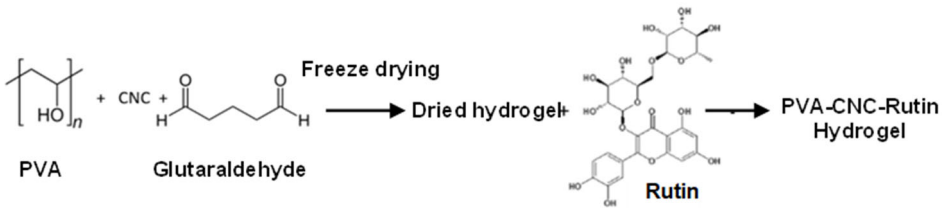

Fig 6. Synthesis of PVA-CNC-rutin hydrogel crosslinked with glutaraldehyde

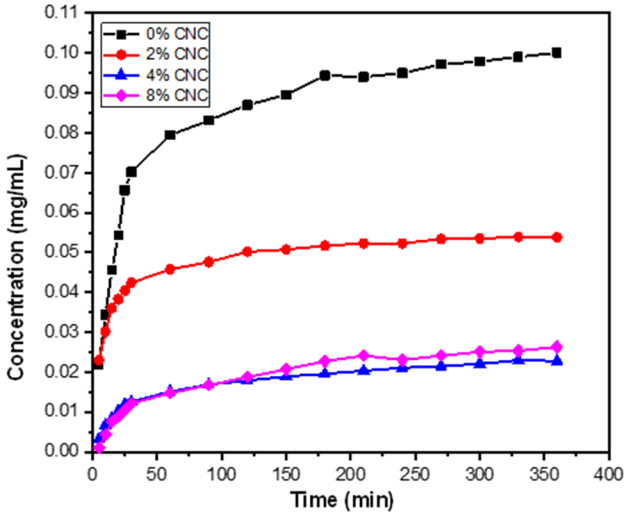

Fig 7. *In vitro* drug release of rutin in PBS pH 7.4, concentration release of rutin versus time

release from the hydrogel network. The 8% CNC showed higher release concentrations than 4% CNC after the first 120 min, and this could be due to the higher concentration of hydroxyl groups of 4% CNC, so the higher entrapment of rutin in 4% CNC was probably due to more and stronger hydrogen bonds with rutin. Further characterization should be conducted.

The *in vitro* rutin-release profiles comprised two phases. The initial one shows significant release and the later steady release. In the first 30 min, rutin was released rapidly (Fig. 7), showing release concentrations of 0.070, 0.042, 0.012 and 0.012 mg/mL for 0, 2, 4, and 8% CNC, respectively. This sudden release might be attributed to rutin near the hydrogel surface and the big difference in concentration between the hydrogel surface and PBS solution, resulting in great diffusion. The total rutin that was released from the hydrogels was 2.530, 1.376, 0.571, and 0.647 mg/mL, respectively. The low concentrations might be due to the poor solubility of rutin in water [35]. The drug release profile of hydrogel is influenced by the solubility of the drug, swelling ability of the hydrogel, and drug-hydrogel interactions [36].

Overall, all hydrogels had a similar release profile for diclofenac sodium, which was uncontrolled release behavior. Diclofenac sodium was released in high concentrations in the first 90 min, then gradually dropped. Compared to rutin, with 10 hydrogen bond donors and 16 hydrogen bond acceptors, diclofenac sodium only has 1 hydrogen bond donor and 3 hydrogen bond acceptors [37]. Diclofenac sodium has weaker links or associations with CNC hydrogel's negatively charged carboxylate ions. Therefore, diclofenac sodium is released early and uncontrollably in PBS solution. The total weight of diclofenac sodium from the lowest to the greatest was in 0, 2, 8, 4, and 6% CNC hydrogel. This result was inversely proportional with the rutin-loaded hydrogels, where a higher CNC concentration resulted in a lower total weight of the drug released.

■ CONCLUSION

In this work, CNC reinforced PVA hydrogels containing active anti-inflammatory agents were prepared. Sodium diclofenac and rutin were employed as drug models. Hydrogels containing rutin showed controlled release properties, but hydrogel with diclofenac sodium performed non-controlled properties with high concentration release between 0 to 90-min incubation. The rutin release profile of 0% CNC showed the highest release concentration, whereas CNC containing hydrogels decreased significantly with the addition of CNC. However, 0% CNC hydrogel showed a distinct high concentration in the beginning compared with other samples comprising CNC. It was shown in this study that the addition of CNC to hydrogels can change their properties, such as tensile strength, Young's modulus, swelling ratio, loading content, and drug release behavior. Besides that, rutin and diclofenac sodium had different release profiles because rutin was better entrapped in the hydrogel. The addition of various concentrations of CNC into PVA hydrogels can result in tuneable drug release properties and potential to be applied in wound dressing. Noteworthy, the selection of active agents must be considered as it will contribute to the molecular interaction with CNC and further influence the drug release profile.

■ ACKNOWLEDGMENTS

The authors gratefully acknowledge financial support from Research, Community Service and Innovation Program, Institut Teknologi Bandung.

■ AUTHOR CONTRIBUTIONS

LATWA: conceptualization, investigation, methodology, writing – review and editing, project administration; AA: experiment, investigation, methodology, writing; YEK: experiment, investigation, methodology; DP; writing – review and editing; UT: methodology, writing – review and editing; HA: writing – review and editing.

■ REFERENCES

[1] Kujath, P., and Michelsen, A., 2008, Wounds-from physiology to wound dressing, *Dtsch. Arztebl. Int.*, 105 (13), 239–248.

[2] de Oliveira Gonzalez, A.C., Costa, T.F., Andrade, Z.A., and Medrado, A.R.A.P., 2016, Wound healing - A literature review, *An. Bras. Dermatol.*, 91 (5), 614–620.

[3] Guo, S., and DiPietro, L.A., 2010, Factors affecting wound healing, *J. Dent. Res.*, 89 (3), 219–229.

[4] Zhang, J.M., and An, J., 2007, Cytokines, inflammation and pain, *Int. Anesthesiol. Clin.*, 45 (2), 27–37.

[5] Negut, I., Grumezescu, V., and Grumezescu, A.M., 2018, Treatment strategies for infected wounds, *Molecules*, 23 (9), 2392.

[6] Edwards, R., and Harding, K.G., 2004, Bacteria and wound healing, *Curr. Opin. Infect. Dis.*, 17 (2), 91–96.

[7] Heyer, K., Augustin, M., Protz, K., Herberger, K., Spehr, C., and Rustenbach, S.J., 2013, Effectiveness of advanced versus conventional wound dressings on healing of chronic wounds: Systematic review and meta-analysis, *Dermatology*, 226 (2), 172–184.

[8] Kumar, A., and Jaiswal, M., 2016, Design and *in vitro* investigation of nanocomposite hydrogel based in situ spray dressing for chronic wounds and synthesis of silver nanoparticles using green chemistry, *J. Appl. Polym. Sci.*, 133 (14), 43260.

[9] Dhivya, S., Padma, V.V., and Santhini, E., 2015, Wound dressings - A review, *Biomedicine*, 5 (4), 22.

[10] Koehler, J., Brandl, F.P., and Goepferich, A.M., 2018, Hydrogel wound dressings for bioactive treatment of acute and chronic wounds, *Eur. Polym. J.*, 100, 1–11.

[11] Wardhani, R.A.K., Asri, L.A.T.W., Rachmawati, H., Khairurrijal, K., and Purwasasmita, B.N., 2020, Physical–chemical crosslinked electrospun *Colocasia esculenta* tuber protein–chitosan–poly(ethylene oxide) nanofibers with antibacterial activity and cytocompatibility, *Int. J. Nanomed.*, 15, 6433–6449.

[12] Hanif, W., Hardiansyah, A., Randy, A., and Asri, L.A.T.W., 2021, Physically crosslinked PVA/graphene-based materials/aloe vera hydrogel with antibacterial activity, *RSC Adv.*, 11 (46), 29029–29041.

[13] Wardhani, R.A.K., Asri, L.A.T.W., Rachmawati, H., Khairurrijal, K., and Purwasasmita, B.S., 2019, Stabilization of chitosan-polyethylene oxide electrospun nanofibrous containing *Colocasia esculenta* tuber protein, *Mater. Res. Express*, 6 (11), 1150f4.

[14] Zheng, C., Liu, C., Chen, H., Wang, N., Liu, X., Sun, G., and Qiao, W., 2019, Effective wound dressing based on Poly (vinyl alcohol)/Dextran-aldehyde composite hydrogel, *Int. J. Biol. Macromol.*, 132, 1098–1105.

[15] Tavakoli, S., and Klar, A.S., 2020, Advanced hydrogels as wound dressings, *Biomolecules*, 10 (8), 1169.

[16] Wang, M., Xu, L., Hu, H., Zhai, M., Peng, J., Nho, Y., Li, J., and Wei, G., 2007, Radiation synthesis of PVP/CMC hydrogels as wound dressing, *Nucl. Instrum. Methods Phys. Res., Sect. B*, 265 (1), 385–389.

[17] Singh, D., Singh, A., and Singh, R., 2015, Polyvinyl pyrrolidone/carrageenan blend hydrogels with nanosilver prepared by gamma radiation for use as an antimicrobial wound dressing, *J. Biomater. Sci., Polym. Ed.*, 26 (17), 1269–1285.

[18] Chen, S.L., Fu, R.H., Liao, S.F., Liu, S.P., Lin, S.Z., and Wang, Y.C., 2018, A PEG-based hydrogel for effective wound care management, *Cell Transplant.*, 27 (2), 275–284.

[19] Liu, S., Jiang, T., Guo, R., Li, C., Lu, C., Yang, G., Nie, J., Wang, F., Yang, X., and Chen, Z., 2021, Injectable and degradable PEG hydrogel with antibacterial performance for promoting wound healing, *ACS Appl. Bio Mater.*, 4 (3), 2769–2780.

[20] Xu, Q., Ji, Y., Sun, Q., Fu, Y., Xu, Y., and Jin, L., 2019, Fabrication of cellulose nanocrystal/chitosan

hydrogel for controlled drug release, *Nanomaterials*, 9 (2), 253.

[21] Leung, A.C.W., Hrapovic, S., Lam, E., Liu, Y., Male, K.B., Mahmoud, K.A., and Luong, J.H.T., 2011, Characteristics and properties of carboxylated cellulose nanocrystals prepared from a novel one-step procedure, *Small*, 7 (3), 302–305.

[22] Tanpichai, S., and Oksman, K., 2016, Cross-linked nanocomposite hydrogels based on cellulose nanocrystals and PVA: Mechanical properties and creep recovery, *Composites, Part A*, 88, 226–233.

[23] George, J., and Sabapathi, S.N., 2015, Cellulose nanocrystals: Synthesis, functional properties, and applications, *Nanotechnol., Sci. Appl.*, 8, 45–54.

[24] Phanthong, P., Reubroycharoen, P., Hao, X., Xu, G., Abudula, A., and Guan, G., 2018, Nanocellulose: Extraction and application, *Carbon Resour. Convers.*, 1 (1), 32–43.

[25] Dong, S., Bortner, M.J., and Roman, M., 2016, Analysis of the sulfuric acid hydrolysis of wood pulp for cellulose nanocrystal production: A central composite design study, *Ind. Crops Prod.*, 93, 76–87.

[26] Lu, Z., Fan, L., Zheng, H., Lu, Q., Liao, Y., and Huang, B., 2013, Preparation, characterization and optimization of nanocellulose whiskers by simultaneously ultrasonic wave and microwave assisted, *Bioresour. Technol.*, 146, 82–88.

[27] Cui, S., Zhang, S., Ge, S., Xiong, L., and Sun, Q., 2016, Green preparation and characterization of size-controlled nanocrystalline cellulose via ultrasonic-assisted enzymatic hydrolysis, *Ind. Crops Prod.*, 83, 346–352.

[28] Isogai, A., and Zhou, Y., 2019, Diverse nanocelluloses prepared from TEMPO-oxidized wood cellulose fibers: Nanonetworks, nanofibers, and nanocrystals, *Curr. Opin. Solid State Mater. Sci.*, 23 (2), 101–106.

[29] Saghazadeh, S., Rinoldi, C., Schot, M., Kashaf, S.S., Sharifi, F., Jalilian, E., Nuutila, K., Giatsidis, G., Mostafalu, P., Derakhshandeh, H., Yue, K., Swieszkowski, W., Memic, A., Tamayol, A., and Khademhosseini, A., 2018, Drug delivery systems and materials for wound healing applications, *Adv. Drug Delivery Rev.*, 127, 138–166.

[30] Asri, L.A.T.W., Rahmatika, A., Fahreza, M.Z., Insanu, M., and Purwasasmita, B.S., 2018, Preparation and release behavior of carboxylated cellulose nanocrystals-alginate nanocomposite loaded with rutin, *Mater. Res. Express*, 5 (9), 095303.

[31] Cheng, M., Qin, Z., Liu, Y., Qin, Y., Li, T., Chen, L., and Zhu, M., 2014, Efficient extraction of carboxylated spherical cellulose nanocrystals with narrow distribution through hydrolysis of lyocell fibers by using ammonium persulfate as an oxidant, *J. Mater. Chem. A*, 2 (1), 251–258.

[32] Oun, A.A., and Rhim, J.W., 2018, Isolation of oxidized nanocellulose from rice straw using the ammonium persulfate method, *Cellulose*, 25 (4), 2143–2149.

[33] Santmartí, A., and Lee, K.Y., 2018, "Crystallinity and Thermal Stability of Nanocellulose" in *Nanocellulose Sustainability*, CRC Press, Boca Raton, Florida, US, 67–86.

[34] Dufresne, A., 2013, Nanocellulose: A new ageless bionanomaterial, *Mater. Today*, 16 (6), 220–227.

[35] Pivec, T., Kargl, R., Maver, U., Bračič, M., Elschner, T., Žagar, E., Gradišnik, L., and Stana Kleinschek, K., 2019, Chemical structure–Antioxidant activity relationship of water–based enzymatic polymerized rutin and its wound healing potential, *Polymers*, 11 (10), 1566.

[36] Dai, H., Zhang, H., Ma, L., Zhou, H., Yu, Y., Guo, T., Zhang, Y., and Huang, H., 2019, Green pH/magnetic sensitive hydrogels based on pineapple peel cellulose and polyvinyl alcohol: synthesis, characterization and naringin prolonged release, *Carbohydr. Polym.*, 209 (381), 51–61.

[37] National Center for Biotechnology Information, 2022, *PubChem Compound Summary for CID 5018304, Diclofenac sodium*, https://pubchem.ncbi.nlm.nih.gov/compound/Diclofenac-sodium, accessed on 10 September 2021.